Facile synthesis of chirality-induced magnetite nanoparticle using mandelic acid

MinJae Kim

February 12, 2022

Abstract

1 Introduction

Owing to its great magnetic properties and biocompatibility, magnetite has received vast attention as platforms for drug delivery[1], magnetic imaging[2], and hyperthermia[3]. Precise control of the bioabsorability and penetrance to the biomembranes is achieved by introducing a plethora of biomolecules including both small molecules, citric acid[4] and oleic acid[5] for instance, and macromolecules such as glucose oxidase[6]. Amongst aforementioned molecules, citric acid and oleic acid do not only act as the origin of the biocompatibilizer, but also a surfactant, in which relative amount affects the morphology and size of the nanoparticles[7][8].

Meanwhile, inspired by the innate chirality of nature, many trials to apply chirality to nanostructures have proceeded past few years. For example, chiral cobalt oxide nanoparticles were synthesized and its *in vivo* enantioselective interaction was reported by *Yeom, et al.*[9]. In an aforementioned case, surprisingly, the chirality of surfactant, cysteine, was propagated to the shell of nanoparticle, resulting in the direction-selective lattice distortion[10]. Besides, variety of chiral metal and their oxide nanoparticles including silver[11], gold[12], and titania[13] were reported.

However, despite its supreme properties including magnetism as well as biocompatibility, the synthesis of chiral magnetite nanoparticles has not been reported. Inspired by siderophores, the facile synthesis of chiral magnetite nanoparticles was reported here. Used chiral surfactant was mandelic acid, an innocuous biomolecule that forms a highly stable Fe(III) complex attributed to the alpha-hydroxy acid group. Thus, mandelic acid-functionalized chiral magnetite nanoparticle is expected to be used widely in the therapeutic field.

2 Methodology

The synthesis of magnetite nanoparticle was typical co-precipitation reported by *Massart, et al.*[14]. The co-precipitation is an innately chemical method, as described following.

$$2\,Fe^{3+} + Fe^{2+} + 8\,OH^- \longrightarrow Fe_3O_4 + 4\,H_2O$$

The stoichiometric ratio between ferric and ferrous ion should be near 2:1, otherwise, it can form other oxide phases such as Fe_2O_3. For instance, it was reported goethite[15] or ferrihydrite[16] are formed if $[Fe^{2+}]/[Fe^{3+}] < 0.1$ and $[Fe^{2+}]/[Fe^{3+}] < 0.35$, respectively. Therefore, ferric and ferrous ion was confined to the ratio of 1:2.

Here, two synthetic ways were applied. The first synthetic way(SCS) was initiated by dissolving 0.450mmol of enantioselective mandelic acid to form a 2.450mL solution of pH$\sim$6. The racemic mixture was manually made by mixing an equimolar amount of R$-$/S$-$ mandelic acid. Then 80μL and 160μL of 1M $FeCl_3{\cdot}6H_2O$ and 1M $FeCl_2{\cdot}4H_2O$ were respectively added to form iron(III) mandelate complex. The pH should be precisely controlled as it has coming and going confinement. If the solution goes to basic(pH$>$7), the aforementioned precipitation reaction will occur while the pH should have a high value within the acidic condition as ionization of α-hydroxyl group should be preceded before chelation of mandelate[17]. The 500μL of 1M Na_2CO_3 was added while vigorous stirring to induce phase transforms to mandelate-functionalized green rust. Then, another 500μL of the solution mentioned earlier was added 5 minutes after the first injection to induce further phase transformation to magnetite nanoparticle. All of the synthesis was performed at a designated temperature. This two-step approach was available owing

to the nature of carbonate, a weak base, that induce slow chemical reaction[18]. After a designated time, 200μL of the sample was aliquoted from the mother solution, and 1mL of ethanol was added, followed by a couple of washing processes including centrifugation at 6200rpm for 1 minute and decantation. This washing process shows similar results with magnetic decantation, here the centrifugation was used for convenience.

In a second way(SHS), 150μL of 5M NaCl was added to 2.3mL of DI water to slow down the formation of magnetite phase by making the time of system that remains in intermediate iron oxide phases long[19]. Then, 100μL and 50μL of 1M $FeCl_3 \cdot 6H_2O$ and 1M $FeCl_2 \cdot 4H_2O$ were respectively added to the solution. In order to precipitate magnetite, 600μL of 1M NaOH solution was added, which color of the solution immediately changed to black. All the synthesis procedures were at 70 °C. After 30 minutes from the base injection, 1mL of the sample was aliquoted and 200μL of 1M HCl solution was added. Then the solution was centrifuged at 6200rpm for 5 minutes, followed by decantation and replenishment of 1mL DI water then centrifugation in the same condition repeated a couple of times. All the precipitation were confirmed optically that the major phase is magnetite and re-dispersed in 1mL of DI water for further use.

3 Results and Discussions

3.1 CD spectra of iron-mandelate system

To investigate whether mandelic acid-functionalized magnetite nanoparticles were sythesized properly, CD spectroscopy were performed for three kinds of system: S-mandelato iron(III), S-mandelato iron(II), and sodium mandelate. All solution were titrated to pH∼7 to exclude any environmental difference with other samples that are described below. The CD spectrum were shown in figure 1, 2, and 3.

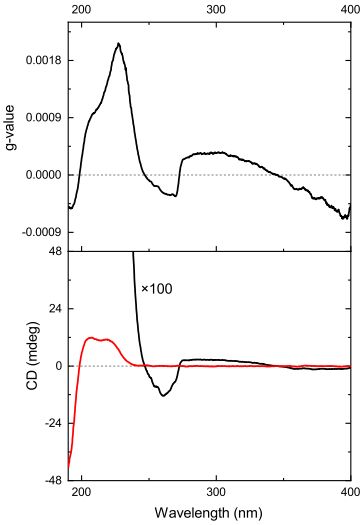

Figure 1: Circular dichroism(CD) spectra of S-mandelato iron(II) complex at pH∼7

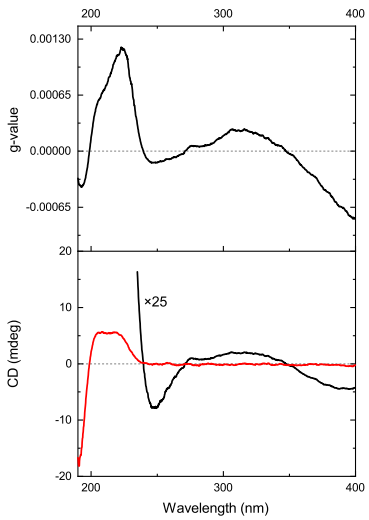

Figure 2: Circular dichroism(CD) spectra of S-mandelato iron(III) complex at pH∼7

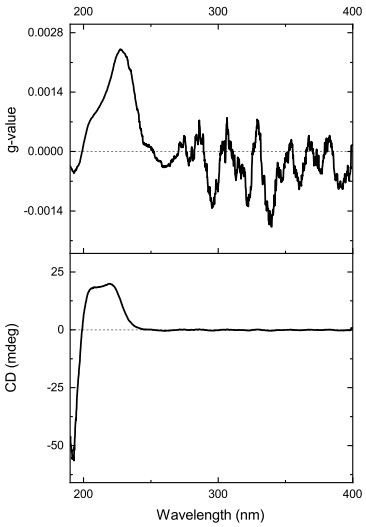

Figure 3: Circular dichroism(CD) spectra of sodium s-mandelate at pH∼7

Notable peaks were observed in each spectra. Peaks near ∼266nm and ∼300nm were observed in s-mandelato iron(II) solution, while peaks ∼245nm and ∼310nm in s-mandelato iron(III) solution. Unfortunately, it was not able to obtain noise-excluded CD spectra of sodium mandelate at pH∼7 in range of $\lambda > 270nm$. These peaks seem to be attributed to induced-chirality of bidentate complex, that enantioselective chelator prefer one of $\Delta - /\Lambda-$complex selectively, which might be due to enantioselective steric hindrance, thus results in other peaks different from that of pure sodium mandelate. One significant peak was observed at ∼260nm in the spectra of sodium mandelate solution. These peaks are especially important for determining whether these species are present in the solution. Here, we observed no peaks at these position were arose in any other CD spectrum of mandelic acid-functionalized magnetite nanoparticles described below, therefore the possibility that mandelato iron(II or III) detection could be excluded.

3.2 Binding mode depending on the synthetic methodology

Two synthetic approaches were adopted to test synthesis methodology. Magnetite nanoparticles which chirality originated from enantioselective mandelic acid were successfully synthesized via both SCS and SHS pathways. Their circular dichroism(CD) spectrum and g-values calculated with equation 1. was shown in figure 4 and 5.

$$g - value = \frac{CD}{Abs \times 32980} \tag{1}$$

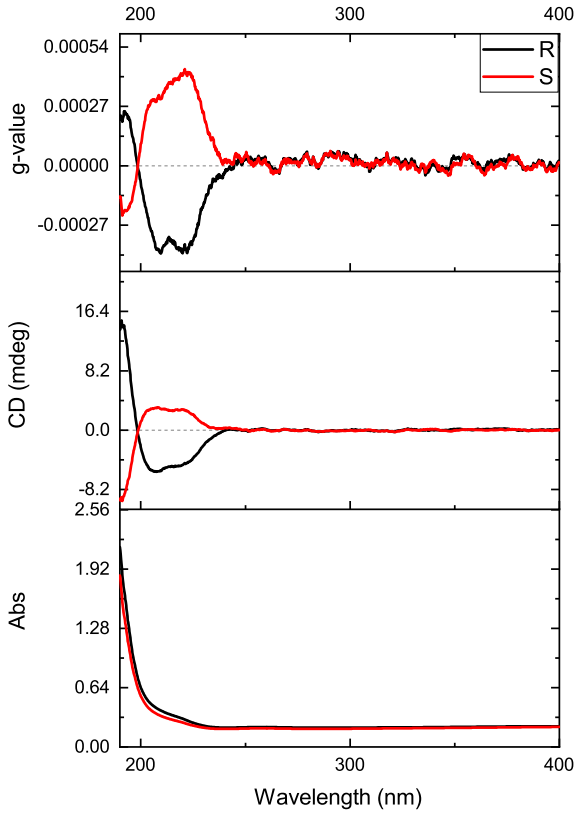

Figure 4: Circular dichroism(CD) spectra of mandelic acid-functionalized magnetite nanoparticle synthesized by SCS method

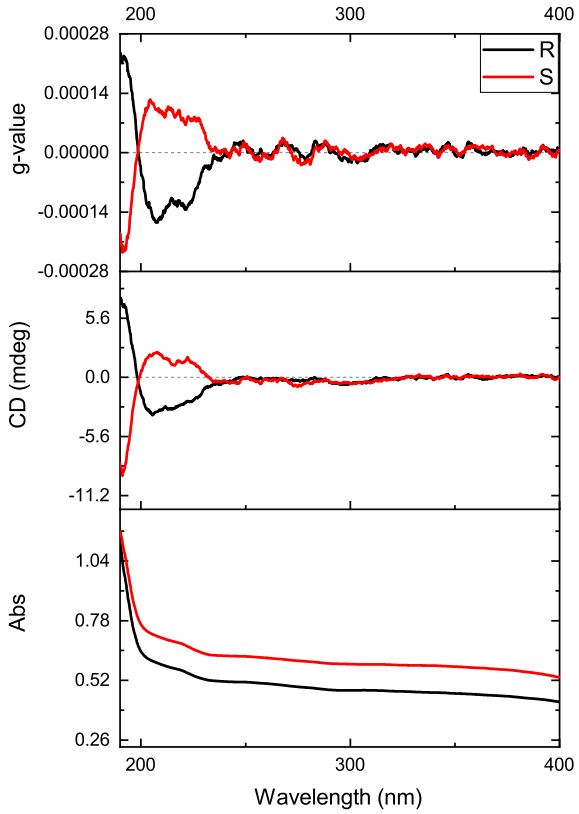

Figure 5: Circular dichroism(CD) spectra of mandelic acid-functionalized magnetite nanoparticle synthesized by SHS method

The characteristic three peaks were observed in both spectrum, that are at ∼193nm, ∼208nm, and ∼223nm. These appearances of known peaks indicate the presence of mandelic acid on the surface of magnetite nanoparticles. Subtle redshift of the peaks, that peaks were reported to appear at ∼190nm, ∼205nm, and ∼220nm, seems to be attributed to stabilization of mandelate by the iron cation. It was reported that these three peaks are respectively assigned to $\pi \rightarrow \pi*$ transition of aromatic ring with charge-transfer character to carboxylic group, $\pi \rightarrow \pi*$ transition of the aromatic ring itself, and $n \rightarrow \pi*$ transition of carboxylic group[20]. Therefore, the binding character can be inferred from the relative strength of the peaks. Amongst them, the relative strength of the peak at ∼193nm is directly related to the strength of Fe(III)-mandelate binding. As it is the only peak related to the electron transition from the non-binding region to the alpha-carboxylic acid part that participates in the binding. The relative prevalence of the peak at ∼193nm compared to peaks at ∼208nm and ∼223nm than them of pure mandelic acid, therefore, suggests a higher covalent bonding character of iron-mandelic acid bond[20]. It should be noted that either SCS and SHS samples show prevailing ∼193nm peaks than pristine mandelic acid.

There is also an enhancement in the intensity of the peak at ∼223nm, which is related to the excitation of electrons from the non-bonding orbital to the anti-bonding orbital. This implies increased localization character of the hybridized electron, results in lower charge-charge interaction between magnetite surface and the mandelic acid. Therefore, this supports the stronger binding of mandelic acid on the magnetite nanoparticle synthesized by the SHS method.

The higher covalency of the mandelic acid-magnetite bond might be attributed to the kinetics of green rust formation. In the SCS process, the system undergoes a green rust phase at least 5 minutes, a time interval between two Na_2CO_3 injection, which might be longer than that of the SHS process, resulting in

a higher breakaway of mandelate ion due to the highly negative atmosphere near ferric and ferrous ion due to the chloride ion and oxygen anion.

3.3 Growth time dependent binding character

The growth time, duration from the first injection of the base in the SCS method was adjusted to investigate the covalency of the iron-mandelate bond depending on the size of the nanoparticle. As the peak at ∼208nm may less be affected by the presence of ferric and ferrous iron than other peaks, the covalency of the samples was compared quantitatively by the ratio between the intensity of two peaks respectively at ∼193nm(I_3) and ∼208nm(I_1). The results were shown in table 1.

Growth time(min)	30	60	120	180
I_3/I_1	0.948	0.978	0.815	0.891

Table 1: Relative intensity of peaks at ∼190nm and ∼207nm

It is notable that all the values in table 1 were saliently higher than that of NaOH-titrated mandelic acid solution(pH∼7) as well as pure mandelic acid solution, which values are $I_3/I_1 = 0.386$ and $I_3/I_1 \sim 0.1$[20], respectively. In pure mandelic acid solution, the lowest I_3/I_1 value was obtained, which is attributed to the least charge transfer to stabilizing cation(H^+). In NaOH titrated mandelic acid including solution, which CD spectra was shown in figure 6, significantly higher values were observed, on the other hand, that Na^+ ion draws a significant amount of charge from mandelate, thus give more covalency. Therefore, it can be concluded that these results may indicate the presence of strong interaction between magnetite surface and mandelate. Meanwhile, no tendency of covalency character I_3/I_1 was observed depnending on the growth time. This implies that characterization of mandelate is mainly arise at the incipient phase of the reaction.

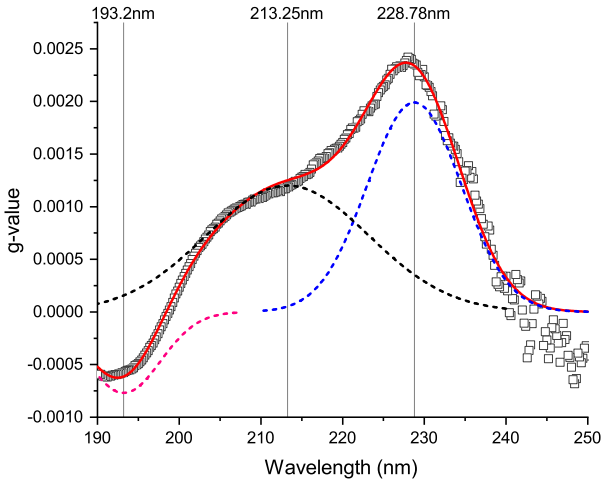

Figure 6: Deconvolution of CD spectra of S-mandelic acid solution at pH=7

The I_3/I_1 values does not show significant tendency depending on the growth time. This might be attributed to either chemical nature of mandelate that its binding on the magnetite surface does not saliently affected by the curvature of the surface or growth inhibition at the incipient phase of magnetite transition that the growth of the nanoparticles becomes negligible. Unfortunately, it was not able to test this hypothesis directly via electron microscopy. Nevertheless, it should be noted that the covalency of the mandelate-magnetite bond is notably high.

3.4 Temperature dependent binding character

To assess temperature dependence of binding character, 10 minutes quick synthesis were performed at various temperature. Na_2CO_3 solution was injected in a step, unlike other almost. Typical color change from transparent orange to turbid dark green followed by black was observed in way faster manner in samples synthesized at higher temperature. Relative intensity of samples were shown in table 2. Unfortunately, synthesis at lower temperature than 50 °C was not available within 10 minutes as reported[18].

Growth Temperature(°C)	50	60	70	80
I_3/I_1	1.314	1.145	1.027	0.889

Table 2: Relative intensity of peaks at ∼193nm, ∼208nm, and ∼223nm

One notable thing is the I_3/I_1 values were much higher than that in table 1. This may be attributed to insufficiently endowed growth time, that remained both mandelato-iron(II) and mandelato-iron(III) complexes contribute to I_3. As $n \rightarrow \pi*$ transition of carboxylic group entails substantial tugging of electron density near α-hydroxyl group to aromatic ring, this excitation may be prevalent if either strong electron drawing ability of benzene ring and its peripheral atmosphere or highly accumulated negative charge of the oxygen atom of α-hydroxyl group. Since it seems there not exist any chemicals in the system that can significantly affect to the electron cloud of benzene ring, we believe latter hypothesis is more convincing. More dense electron density of the oxygen atom may result in lower covalent character, thus higher coordination character, which shows coincidence with I_3/I_1 values.

The temperature dependence of covalency seems to be originated from competition between the condensation of aquo-complexes and that involving mandelate ion. It is known that the formation of oxo-bridge from aquo-complexes is saliently favored at high temperature, therefore results in faster kinetics of the precipitation[18]. This results in less opportunity of mandelate to participate in nucelophilic attack, thus less amount of sorbed mandelate.

3.5 Superfast synthesis of mandelate-functionalized magnetite nanoparticle

From the observation that phase transformation to magnetite was significantly fast at high temperature, superfacile synthesis of magnetite nanoparticle was proceeded here. The base solution was added in once and the solution was agitated for 5 minutes. This availability of superfast synthesis supports a aforementioned hypothesis that describes the mandelate functionalization take place in early stage of reaction. Measured CD spectra was shown in figure 7.

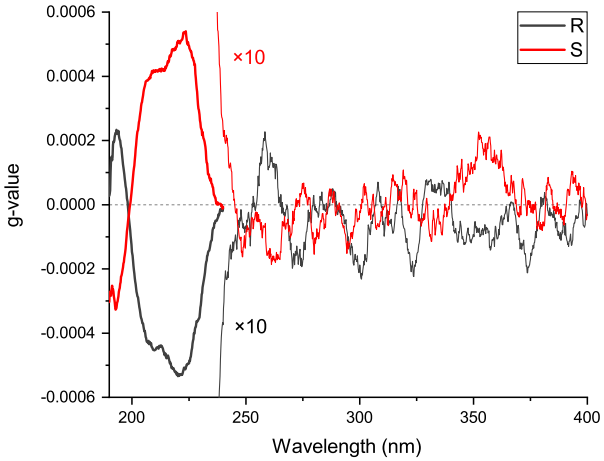

Figure 7: CD spectra of mandelic acid-functionalized magnetite nanoparticles synthesized by superfast way.

Small peaks were observed at ∼260nm and ∼360nm. It was reported small peak at ∼260nm is assigned to $\pi \rightarrow \pi*$ transition[18]. On the other hand, peak at ∼360nm is expected to be arose from the subtle distortion of the lattice, as its energy is too low to be assigned to the electron transition within the mandelic acid molecule. Unfortunately, it was not able to conform this hypothesis.

4 Conclusion

The chirality was endowed to magnetite nanoparticle by functionalization with chiral mandelic acid. The covalency of iron-mandelate bonds were compared via ratio between intensity of two characteristic peaks. Both synthetic method and the temperature made different covalency, while the growth time, thus size, does not. These results were explained by the temperature dependent kinetics of magnetite precipitation. Owing to their good magnetic properties and chirality, this can be used for various applications including

magnetic resonance imaging and drug delivery. However, experimental investigation of *in vivo* activities of the nanoparticles was not examined here.

References

[1] Guo, Shaojun, et al. "Monodisperse mesoporous superparamagnetic single-crystal magnetite nanoparticles for drug delivery." *Biomaterials* 30.10 (2009): 1881-1889.

[2] Haw, Choon Yian, et al. "Hydrothermal synthesis of magnetite nanoparticles as MRI contrast agents." *Ceramics International* 36.4 (2010): 1417-1422.

[3] Kobayashi, Takeshi. "Cancer hyperthermia using magnetic nanoparticles." *Biotechnology journal* 6.11 (2011): 1342-1347.

[4] Răcuciu, Mihaela, D. E. Creangă, and Anton Airinei. "Citric-acid-coated magnetite nanoparticles for biological applications." *The European Physical Journal E* 21.2 (2006): 117-121.

[5] Zhang, Ling, Rong He, and Hong-Chen Gu. "Oleic acid coating on the monodisperse magnetite nanoparticles." *Applied Surface Science* 253.5 (2006): 2611-2617.

[6] Rossi, Liane M., Ashley D. Quach, and Zeev Rosenzweig. "Glucose oxidase–magnetite nanoparticle bioconjugate for glucose sensing." *Analytical and Bioanalytical Chemistry* 380.4 (2004): 606-613.

[7] Dheyab, Mohammed Ali, et al. "Simple rapid stabilization method through citric acid modification for magnetite nanoparticles." *Scientific reports* 10.1 (2020): 1-8.

[8] Sun, Shouheng, and Hao Zeng. "Size-controlled synthesis of magnetite nanoparticles." *Journal of the American Chemical Society* 124.28 (2002): 8204-8205.

[9] Yeom, Jihyeon, et al. "Chiral supraparticles for controllable nanomedicine." *Advanced Materials* 32.1 (2020): 1903878.

[10] Yeom, Jihyeon, et al. "Chiromagnetic nanoparticles and gels." *Science* 359.6373 (2018): 309-314.

[11] Shemer, Gabriel, et al. "Chirality of silver nanoparticles synthesized on DNA." *Journal of the American Chemical Society* 128.34 (2006): 11006-11007.

[12] Lee, Hye-Eun, et al. "Amino-acid-and peptide-directed synthesis of chiral plasmonic gold nanoparticles." *Nature* 556.7701 (2018): 360-365.

[13] Cleary, Olan, et al. "Chiral and luminescent TiO2 nanoparticles." *Advanced Optical Materials* 5.16 (2017): 1601000.

[14] Massart, Rene. "Preparation of aqueous magnetic liquids in alkaline and acidic media." *IEEE transactions on magnetics* 17.2 (1981): 1247-1248.

[15] Tronc, Elisabeth, et al. "Transformation of ferric hydroxide into spinel by iron (II) adsorption." *Langmuir* 8.1 (1992): 313-319.

[16] Jolivet, J. P., et al. "Influence of Fe (II) on the formation of the spinel iron oxide in alkaline medium." *Clays and Clay Minerals* 40.5 (1992): 531-539.

[17] Smythe, C. V., and Carl LA Schmidt. "Studies on the mode of combination of iron with certain proteins, amino acids, and related compounds." *Journal of Biological Chemistry* 88.1 (1930): 241-269.

[18] Blanco-Andujar, Cristina, et al. "Elucidating the morphological and structural evolution of iron oxide nanoparticles formed by sodium carbonate in aqueous medium." *Journal of Materials Chemistry* 22.25 (2012): 12498-12506.

[19] Patel, Daksha, Yongmin Chang, and Gang Ho Lee. "Amino acid functionalized magnetite nanoparticles in saline solution." *Current Applied Physics* 9.1 (2009): S32-S34.

[20] Evans, Amanda C., et al. "Chiroptical characterization tools for asymmetric small molecules–experimental and computational approaches for electronic circular dichroism (ECD) and anisotropy spectroscopy." *RSC Advances* 11.3 (2021): 1635-1643.

[21] Ahn, Taebin, et al. "Formation pathways of magnetite nanoparticles by coprecipitation method." *The journal of physical chemistry C* 116.10 (2012): 6069-6076.